Journal of Inorganic Biochemistry 192 (2019) 7–16

Contents lists available at ScienceDirect

Journal of Inorganic Biochemistry

journal homepage: www.elsevier.com/locate/jinorgbio

Synthesis, photodynamic activities, and cytotoxicity of new water-soluble cationic gallium(III) and zinc(II) phthalocyanines

Rei Fujishiro[a], Hayato Sonoyama[a], Yuki Ide[a], Takuya Fujimura[a], Ryo Sasai[a,*], Atsushi Nagai[b], Shigeki Mori[c], Nichole E.M. Kaufman[d], Zehua Zhou[d], M. Graça H. Vicente[d], Takahisa Ikeue[a,*]

[a] Department of Chemistry, Graduate School of Science and Engineering, Shimane University, 1060 Nishikawatsu, Matsue 690-8504, Japan
[b] Department of Laboratory Medicine, Shimane University School of Medicine, Izumo, Japan
[c] Advanced Research Support Center, Ehime University, 2-5 Bunkyo-cho, Matsuyama 790-8577, Japan
[d] Department of Chemistry, Louisiana State University, Baton Rouge, LA 70803-1804, USA

ARTICLE INFO

Keywords:
Phthelocyanine
Water-soluble
Singlet oxygen
PDT

ABSTRACT

The cationic Ga(III) and Zn(II) phthalocyanines carrying *N*-methyl-pyridinium groups at eight peripheral β-positionshave been synthesized. These complexes are highly soluble in dimethyl sulfoxide (DMSO) and moderately soluble in water and phosphate buffered saline (PBS); both Ga(III)Cl and Zn(II) complexes have shown no aggregation in water up to 1.2×10^{-4} and 1.5×10^{-5} M, respectively. A higher water-solubility of Ga(III)Cl complex as compared to Zn(II) complex is ascribed to the presence of an axially coordinated chloride. The spectroscopic properties, photogeneration of singlet oxygen ($^1O_2$), and cytotoxicity of these complexes have been investigated. The absolute quantum yields ($\Phi\Delta_{absolute}$) for the photogeneration of singlet oxygen using Ga(III)Cl and Zn(II) complexes have been determined to be 4.4 and 5.3%, respectively, in DMSO solution. The cytotoxicity and intracellular sites of localization of Ga(III)Cl and Zn(II) complexes have been evaluated in human HEp2 cells. Both complexes, localized intracellularly in multiple organelles, have shown no cytotoxicity in the dark. Upon exposure to a low light dose (1.5 J/cm^2), however, Zn(II) complex has exhibited a high photocytotoxicity. The result suggests that Zn(II) complex can be considered as a potential photosensitizer for Photodynamic therapy (PDT).

1. Introduction

Phthalocyanines (Pcs) and their metal complexes have attracted much attention because of their characteristic physicochemical properties ascribed to their expanded π-conjugation system [1]. One of such characteristics is their intensive absorption band in the near-IR region, called as the Q-band, with a typical molar extinction coefficient (ε) of ca. $10^5\,M^{-1}\,cm^{-1}$. Pcs and their metal complexes have multiple applications such as photoconductivity agents in photocopying machines and dye-sensitized solar cells in photovoltaics [2–3]. Furthermore, the development of Pcs and their metal complexes as photosensitizers in photodynamic therapy (PDT) for cancer and other diseases is a particularly active research field since PDT is a very important and promising methodology already in use in many countries [4–7]. The reactive oxygen species (ROS) such as singlet oxygen ($^1O_2$) and free radicals generated during PDT treatment are responsible for killing the cancer cells. Water-soluble Pcs and their metal complexes are promising photosensitizers to be used in PDT, owing to their intensive Q-band in near-IR region (670–750 nm) and their ability for generating ROS upon light activation; near-IR light can penetrate deeply into living tissues [8–10]. However, most of the water-soluble Pcs containing hydrophilic groups around the Pc core show strong molecular aggregations in aqueous media, which weakens the molar absorption coefficient of the absorption band and consequently decreases the $^1O_2$ generation. To minimize Pc aggregation and to increase their photodynamic activity, several amphiphilic groups and bulky axial ligands have been introduced at the macrocycle periphery and the metal site, respectively [11–13]. Of particular interest are positively charged Pcs, since such molecules should target highly vulnerable intracellular sites and cause an effective DNA photodamage [14–16]. Furthermore, positively charged Pcs have been successfully used for the photoinactivation of Gram-negative and -positive bacteria [17–19].

Because of the unique properties of positively charged Pcs, the novel cationic Pcs including pyridinium substituted phthalocyanines still have been synthesized and researched [20–22].

Among the cationic Pcs, those containing pyridinium groups are

* Corresponding authors.
E-mail addresses: rsasai@riko.shimane-u.ac.jp (R. Sasai), ikeue@riko.shimane-u.ac.jp (T. Ikeue).

https://doi.org/10.1016/j.jinorgbio.2018.11.013
Received 26 September 2018; Received in revised form 19 November 2018; Accepted 21 November 2018
Available online 05 December 2018
0162-0134/

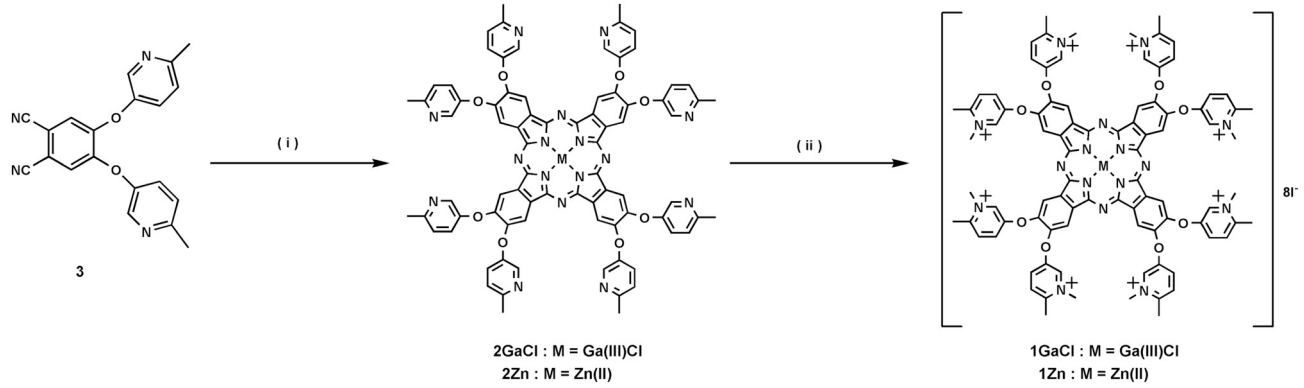

Scheme 1. Synthesis of phthalocyanine complexes. (i) DBU, *n*-pentanol, 145 °C, 24 h; (ii) CH_3I, 45 °C, 24 h.

particularly interesting, since these complexes can be easily obtained by the alkylation of the pyridyl nitrogen atoms. We have previously reported the synthesis of Si(IV) and Zn(II) Pcs bearing pyridyloxy groups at eight peripheral *β*-positions and bulky axial ligands at the metal site and converted them to the corresponding water-soluble cationic complexes by the *N*-methylation of pyridyl nitrogen atoms. They have shown less aggregation in aqueous media such as water and phosphate buffered saline (PBS) solutions [23].

To obtain further examples of cationic Pcs showing no aggregation in aqueous media, synthesis of new water-soluble cationic Ga(III) and Zn(II) complexes have been planned, as shown in Scheme 1. Herein, we report the synthesis, spectroscopic properties, and aggregation behavior of these complexes in aqueous media using absorption and fluorescence spectroscopy. We also report the photo-generation of singlet oxygen by means of UV–Vis and ESR spectroscopy together with the reaction mechanism and absolute quantum yield for the formation of singlet oxygen. In the last part of this manuscript, we have discussed the cytotoxicity and intracellular sites of localization of these complexes by using human HEp2 cells. Based on the results of these experiments, we confirmed that Zn(II) complex could be considered as the potential photosensitizer for PDT.

2. Experimental section

2.1. Instrumentation

All solvents and reagents were purchased from commercial sources and used without preparation. All reactions were performed under N_2 atmosphere. Elemental analyses for carbon, hydrogen, and nitrogen were conducted using a Yanako CHN CORDER MT-6. UV–Vis absorption spectra were recorded on a Shimadzu UV-3100 spectrometer. Photoluminescence (PL) spectra were recorded on a Shimadzu RF-5300PC spectrofluorometer. ^{1}H NMR spectra were recorded on a JEOL delta ECX-500 spectrometer operating at 500.1 MHz. Chemical shifts for ^{1}H NMR spectra were referenced to $CDCl_3$ (δ = 7.26 ppm), CD_2Cl_2 (δ = 5.32 ppm) and D_2O (δ = 4.79 ppm). Electrospray ionization mass (ESI-TOF-MS) spectra were recorded on a Bruker microTOF using an acetonitrile solution method with sodium formate as a reference. Matrix-assisted laser desorption/ionization time-of-flight mass (MALDI-TOF-MS) spectra were recorded on a bioMérieux VITEK® MS. Fluorescence quantum yields were evaluated using an absolute PL quantum yield measurement apparatus (C9920-02, Hamamatsu Photonics). A Xenon lamp (Asahi Spectra, MAX-301) was used as a light source to induce photosensitized singlet oxygen evolution reaction. Light intensities were measured with an Optical power meter (ADCMT, 8230E) equipped with an optical sensor (ADCMT, 82311B). EPR spectra were recorded on a Bruker EMX Plus spectrometer operating at room temperature.

2.2. Syntheses

2.2.1. 4,5-bis(4′-methylpyridin-3′-yloxy)phthalonitrile (3)

4,5-Dichlorophthalonitrile (1.0 g, 5.3 mmol) and 5-hydroxy-2-methylpyridine (1.4 g, 12.4 mmol) were dissolved in 15 mL of dry *N*,*N*-dimethylformamide at 80 °C under N_2. Potassium carbonate (4.5 g, 32.6 mmol) was added to the reaction solution in 5 portions every 5 min. The reaction mixture was heated for 3 h at 80 °C, then cooled to room temperature, and poured into 100 mL of ice–water. The title compound was extracted for the reaction liquid using 50 mL of $CHCl_3$ at 3 times. After filtration under vacuum, the title compound was obtained as a white powder. Yield, 1.8 g (97% (based on 4,5-Dichlorophthalonitrile)). *Anal.* Calc. for $C_{20}H_{14}N_4O_2$: C; 70.17, H; 4.12, N; 16.37. Found: C; 69.93, H; 4.21, N; 16.08%. HR-MS (ESI-TOF): Found 343.1190 *m/z*. $[M + H]^+$ (calcd. for $C_{20}H_{14}N_4O_2$ 343.1191). ^{1}H NMR (CD_2Cl_2): δ = 8.31 (s, 2H, Ar-H), 7.34 (d, 2H, *J* = 8.4 Hz, Ar-H), 7.26 (d, 2H, *J* = 8.4 Hz, Ar-H), 7.23 (s, 2H, Ar-H), and 2.57 ppm (s, 6H, CH_3).

2.2.2. 2,3,6,7,10,11,14,15-Octakis-[(4-methyl-3-pyridyloxy) phthalocyaninato] chloro gallium(III) (2GaCl)

A reaction between phthalonitrile **3** (0.45 g, 1.3 mmol) and anhydrous gallium(III) chloride (0.12 g, 0.682 mmol) was induced in *n*-pentanol (10 mL) in the presence of 0.3 mL of 1,8-diazabicyclo[5.4.0] undec-7-ene (DBU) under N_2. The mixture was heated at 145 °C for 24 h and then concentrated under reduced pressure to dry residue. The crude product was redeposited using a methanol / H_2O mixed solution. The precipitate was obtained as a blue-green solid. Yield, 0.40 g (83% (based on phthalonitrile **3**)). *Anal.* Calc. for $C_{80}H_{56}ClGaN_{16}O_8 \cdot H_2O$: C, 64.37; H; 3.92, N; 15.01. Found: C; 64.67, H; 4.05, N; 14.86%. MALDI-TOF: Found 1439.367 *m/z*. $[M - Cl]^+$ (calcd. for $C_{80}H_{56}GaN_{16}O_8$ 1439.371). UV–vis (DMSO): $\lambda_{max}(\varepsilon/mol^{-1}dm^3\,cm^{-1})$ = 356 (8.0×10^4), 370 (9.2×10^4), 617 (4.2×10^4), 655 (3.7×10^4, sh), and 685 nm (2.5×10^5). ^{1}H NMR (CD_2Cl_2): δ = 8.70 (s, 8H, Pc α-H), 8.62 (s, 8H, Py-H), 7.55 (d, *J* = 8.2 Hz, 8H, Py-H), 7.23(d, *J* = 8.4 Hz, 8H, Py-H), and 2.60 ppm (s, 24H, CH_3).

2.2.3. 2,3,6,7,10,11,14,15-Octakis-[(4-methyl-3-pyridyloxy) phthalocyaninato] zinc(II) (2Zn)

Zinc phthalocyanine **2Zn** was synthesized by a same synthetic route of Ga(III)Cl phthalocyanine **2 GaCl**. Phthalonitrile **3** (0.45 g, 1.3 mmol) and zinc acetate dihydrate (0.14 g, 0.64 mmol) were used in macrocyclization reaction. Zinc phthalocyanine **2Zn** was obtained as a blue-

green solid. Yield, 0.28 g (58% (based on Phthalonitrile **3**)). Anal. Calc. for $C_{80}H_{56}N_{16}O_8Zn$: C, 66.97, H; 3.93, N; 15.62. Found: C; 66.88, H; 4.06, N; 15.45%. HR-MS (ESI-TOF): Found 1433.3774 *m/z*. $[M + H]^+$ (calcd. for $C_{80}H_{56}N_{16}O_8Zn$ 1433.3831). UV–vis ($CHCl_3$): $\lambda_{max}(\varepsilon/mol^{-1}dm^3\,cm^{-1})$ = 359 (5.9×10^4), 611 (2.3×10^4), 647 (2.1×10^4, sh), and 677 nm (1.3×10^5). ^1H NMR ($CDCl_3$ + 10% Pyridine-d_5): δ = 8.75 (s, 8H, Ar-H), 8.45 (s, 8H, Py-H), 7.40 (d, J = 8.3 Hz, 8H, Py-H), 7.06 (d, J = 8.4 Hz, 8H, Py-H), and 2.47 ppm (s, 24H, CH_3).

2.2.4. 2,3,6,7,10,11,14,15-Octakis-[N-methyl-(4-methylpyridinium-3-yloxy)phthalocyaninato] chloro gallium(III) iodide (1GaCl)

Gallium(III) chloride phthalocyanine **2GaCl** (0.10 g, 0.068 mmol) and 10 mL of CH_3I were stirred at 45 °C under N_2. After 1 day, CH_3I was removed under reduced pressure. The crude product was washed with acetone to obtain the cationic compound as a green solid. Yield, 0.17 g (90% (based on phthalocyanine **2GaCl**)). *Anal.* Calc. for $C_{88}H_{80}GaClI_8N_{16}O_8 \cdot 2H_2O$: C; 39.94, H; 3.20, N; 8.47. Found: C; 39.65, H; 2.98, N; 8.27%. UV–vis (H_2O): $\lambda_{max}(\varepsilon/mol^{-1}dm^3\,cm^{-1})$ = 359 (8.5×10^4), 612 (3.2×10^4), 652 (3.2×10^4, sh), and 679 nm (2.1×10^5). ^1H NMR (D_2O): δ = 9.37 (s, 8H, Pc α-H), 8.91 (br, 8H, Py-H), 8.40 (br, 8H, Py-H), 7.95 (s, 8H, Py-H), 4.19 ppm (s, 24H, Py-CH_3) and 2.76 ppm (s, 24H, Py-CH_3).

2.2.5. 2,3,6,7,10,11,14,15-Octakis-[N-methyl-(4-methylpyridinium-3-yloxy)phthalocyaninato] zinc(II) iodide (1Zn)

Cationic Zn(II) phthalocyanine **1Zn** was synthesized by a same synthetic route of cationic Ga(III)Cl phthalocyanine **1GaCl**.

Zinc phthalocyanine **2Zn** (0.10 g, 0.070 mmol) and 10 mL of CH_3I were used in quaternization reaction. Cationic Zn(II) phthalocyanine was obtained as a green solid. Yield, 0.12 g (65% (based on phthalocyanine **2Zn**)). *Anal.* Calc. for $C_{88}H_{80}I_8N_{16}O_8Zn \cdot 3H_2O$: C; 40.27, H; 3.30, N; 8.54. Found: C; 40.24, H; 3.12, N; 8.34%. HR-MS (ESI-TOF): Found 729.0312 *m/z*. $[M - 3I]^{3+}$ (calcd. for $[C_{88}H_{80}I_8N_{16}O_8Zn - 3I]^{3+}$ 729.0281). UV–vis (H_2O): $\lambda_{max}(\varepsilon/mol^{-1}dm^3\,cm^{-1})$ = 351 (7.1×10^4), 607 (2.8×10^4), 645 (3.0×10^4, sh), and 673 nm (1.8×10^5). ^1H NMR (D_2O): δ = 8.45 (s, 8H, Ar-H), 7.94 (br, 8H, Py-H), 7.77 (br, 8H, Py-H), 7.40 (s, 8H, Py-H), 4.10 ppm (s, 24H, *m*-CH_3) and 2.63 ppm (s, 24H, *p*-CH_3).

2.3. The singlet oxygen generation

The singlet oxygen generation of **1GaCl** and **1Zn** via photoirradiation was demonstrated in DMSO and PBS solution. Sample solutions in quartz cuvette were irradiated with monochromatic light (670 nm) through a band-pass filter (Asahi Spectra, MX0670) from Xe lump (Asahi Spectra, MAX-300). Sample preparation was carried out in the dark. 1,3-Diphenylisobenzofuran (DPBF) and 9,10-Antracenediyl-bis (methylene) dimalonoic acid (ADMA) were used as scavengers of active oxygen species in DMSO and a PBS solution, respectively. Sample solutions contains 1.5 mL of phthalocyanine solution at 2.0×10^{-6} M and 1.5 mL of singlet oxygen scavenger solution at 2.0×10^{-5} M. The photochemical reactions were followed spectrophotometrically by observing the decrease of absorption peak at 417 nm and 380 nm of DPBF and ADMA, respectively. Quantum yield of decomposition of scavenger ($\Phi\Delta_{absolute}$) was defined as

$$\Phi\Delta_{Absolute} = \frac{(number\ of\ decomposed\ scavenger\ molecule)}{(number\ of\ adsorbed\ photon)} \quad (1)$$

and then number of adsorbed photon was calculated from following equation

$$(number\ of\ adsorbed\ photon) = \frac{\Delta E\lambda}{hc} \quad (2)$$

where ΔE was adsorbed energy calculated from power of irradiated light and transmitted light measured with an Optical power meter (ADCMT, 8230E) equip with an optical sensor (ADCMT, 82311B). λ is wavelength of irradiated light, h is Planck constant and c is speed of light, respectively.

2.4. Cell study

All tissue culture medium and reagents were purchased from Invitrogen (Carlsbad, CA). The HEp2 cells were purchased from ATCC and cultured using 50:50 DMEM/Advanced MEM augmented with 10% fetal bovine serum (FBS) and 1% antibiotic (penicillin-streptomycin). A 32 mM stock solution of each Pc complex was prepared by dissolving in DMSO containing 1% Cremophor EL.

2.4.1. Dark cytotoxicity

The HEp2 cells were plated in a Corning Costar 96-well plate and allowed to grow for 48 h. The 32 mM 1GaCl and 1Zn stock solutions were diluted with culture medium to concentrations of 0, 3.125, 6.25, 12.5, 25, 50, 100 and 200 μM. The cells were treated with the 1GaCl or 1Zn at the different concentrations (100 μL/well), for 24 h at 37 °C. Immediately following incubation the loading medium was removed, and the cells were washed with PBS to remove any residual Pc. The cells were then fed medium containing 20% CellTiter Blue (Madison, WI) and incubated for 4 h. Cell viability was determined by fluorescence intensity at 570/615 nm using a BMG FLUOstar OPTIMA microplate reader. The dark cytotoxicity is expressed as a percentage of viable cells.

2.4.2. Photocytotoxicity

HEp2 cells were plated and allowed to grow as described above. The Pc concentrations used for testing photocytotoxicity were 0, 3.125, 6.25, 12.5, 25, 50 and 100 μM. As for the dark toxicity assay, the cells were treated with each Pc and incubated at 37 °C for 24 h. Immediately following incubation the loading medium was removed and the cells were washed to remove any residual Pc. The cells were then fed fresh medium and exposed to light for 20 min using a 600 W Quartz Tungsten Halogen lamp (Newport Corporation, Irvine CA) to generate a light dose of approximately 1.5 J/cm^2. During light exposure, the plate was chilled using an Echotherm IC50 chilling/heating plate (Torrey Pines Scientific, Carlsbad CA) set to 5 °C to maintain ambient temperature. Following light exposure the cells were incubated for another 24 h, after which the media was removed and replaced with 20% CellTiter Blue and subsequently incubated for 4 h. The cell viability was determined by fluorescence intensity at 570/615 nm using a BMG FLUOstar OPTIMA microplate reader. The cell photocytotoxicity is expressed as a percentage of viable cells.

2.4.3. The intracellular localization of photosensitizers

HEp2 cells were plated in a 35 mm tissue culture dish (CELLTREAT, Pepperell MA) and allowed to grow for 24 h. The cells were then exposed to each Pc at a concentration of 10 μM for 6 h. Organelle tracers were obtained from Invitrogen and used at the following concentrations: LysoSensor Green 50 nM, MitoTracker Green 250 nM, ER Tracker Blue/White 100 nM, and BODIPY FL C5 Ceramide 1 μM. The images were acquired using a Leica DM6B microscope with 40× water objective lens and DAPI, GFP, and Texas Red filter cubes (Chroma Technologies).

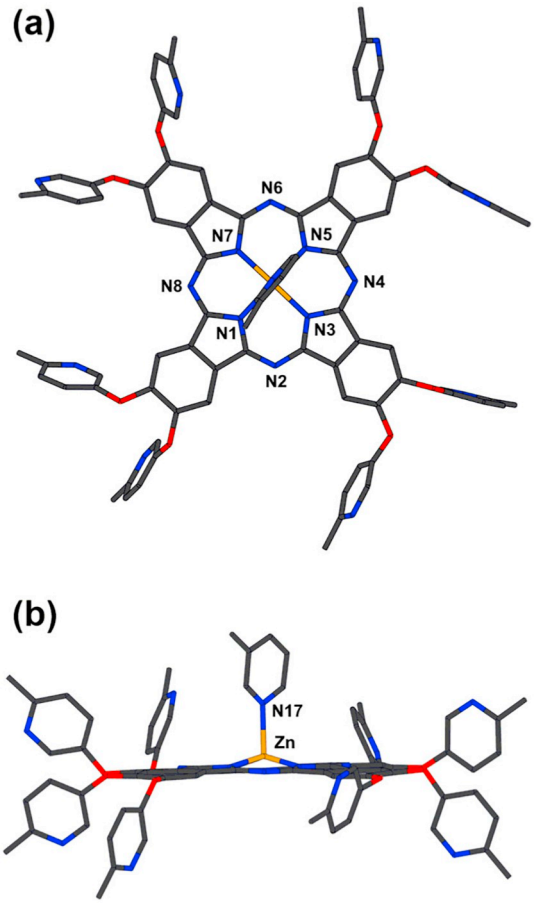

Fig. 1. Crystal structure of **2Zn · (3-Me-Py)$_2$** (a: top view, b: side view). Hydrogen and solvents atoms are omitted for clarity. CCDC number: 1869572.

3. Results and discussion

3.1. Synthesis and characterization

The 4,5-bis(4′-methylpyridin-3′-yloxy)phthalonitrile (**3**) was prepared in 97% yield from commercially available 4,5-dichlorophthalonitrile and 5-hydroxy-2-methylpyridine using the method previously described in the literature [24]. The subsequent macrocyclization and quaternization reactions were achieved by methods described in the literature [23–26]. The neutral Pc complexes **2GaCl** and **2Zn** containing a 4-methylpyridyl group at eight peripheral Pc β -positions were prepared from phthalonitrile **3** and the corresponding metallic salts. These reactions were catalyzed by DBU in anhydrous *n*-propanol, and the isolated yields of complexes **2GaCl** and **2Zn** were 83 and 58%, respectively. Elemental analysis and spectroscopic data (^{1}H NMR and MALDI-TOF mass spectra) confirmed the assigned structures for complexes **2GaCl** and **2Zn**.

The crystal structure of complex **2Zn** · 3-methylpyridine is shown in Fig. 1. The crystal data, bond distances and bond angles are shown in Table S1 and S2 in supporting information. This crystal was obtained by recrystallization of **2Zn** in 3-methylpyridine/hexane. This crystal structure involves 3-methylpyridine coordinating the zinc atom of **2Zn** and co-crystallized 2 molecules of 3-methylpyridine. The peripheral substituents 4-methylpyridyl groups showed no coordination with the zinc atom. The central zinc atom of the Pc adopts five coordination structures, which correspond to the reported structures of zinc(II) Pc complexes axially coordinated by a pyridine molecule [27–30]. The bond length between the N atom (N17) and the zinc atom is 2.108(4) Å. The five N atoms (N1, 3, 5, 7, 17) coordinate in a pyramidal geometry with the zinc atom. The zinc atom also lies 0.453 Å out of the square-plane which is composed by the four Pc inner N atoms (N1, 3, 5, 7) bonded to the central Zn atom.

Quaternization of the 4-methylpyridine groups at the Pc periphery of complexes **2GaCl** and **2Zn** using an excess of methyl iodide (CH_3I) at 40 °C, led to the formation of the cationic Pc complexes **1GaCl** and **1Zn** with yields of 90 and 65%, respectively. After methylation, the cationic complexes **1GaCl** and **1Zn** were highly soluble in DMSO, moderately soluble in water and PBS solutions and slightly soluble in organic solvents, such as dichloromethane and chloroform. Generally, Pc complexes are poorly soluble in most polar and protic solvents. However, the introduction of eight *N*-methyl-pyridinium groups around the Pc macrocycle increases its solubility in polar solvents. Complexes **1GaCl** and **1Zn** were identified by ^{1}H NMR spectroscopy, mass spectrometry and elemental analysis. The analyses are consistent with the assigned structures, as described in the Experimental section. The ESI and MALDI-TOF mass spectra did not show the molecular ion for complex **1GaCl**. The ^{1}H NMR spectra of complexes **1GaCl** and **1Zn** were obtained in D_2O at room temperature. In the ^{1}H NMR spectrum of complex **1GaCl**, the α-proton signal of the Pc ring shows a sharp singlet at δ = 9.37 ppm integrating for 8 protons. The proton signals of the *N*-methyl-(4-methylpyridinium-3-yloxy) groups appear at δ = 8.91, 8.40, and 7.95 ppm, integrating for 8 protons, and their methyl proton signals appear at δ = 4.19 and 2.76 ppm, integrating for 24 protons. On the other hand, in the ^{1}H NMR spectrum of complex **1Zn,** the α-proton signal of the Pc ring shows a sharp singlet at δ = 8.45 ppm integrating for 8 protons. The proton signals for the *N*-methyl-(4-methylpyridinium-3-yloxy) groups appear at δ = 7.94, 7.77 and 7.40 ppm, integrating for 8 protons, and their methyl proton signals appear at δ = 4.10 and 2.63 ppm, integrating for 24 protons.

3.2. Absorption and florescence spectra

The UV–vis and fluorescence spectra of cationic Pcs **1GaCl** and **1Zn** are shown in Fig. 2. The UV–vis and fluorescence spectra were measured in DMSO, water, and PBS solution. At 1.5×10^{-5} M concentration, the Q-bands of **1GaCl** were observed as a sharp absorption in DMSO and water, respectively, at 681 and 679 nm. At 1.5×10^{-5} M concentration, the Q-bands of **1Zn** were observed as a sharp absorption in DMSO and water, respectively at 678 and 673 nm. The fluorescence emission of complex **1GaCl** appeared at 684 and 685 nm and the absolute fluorescence quantum yield (ΦF) of complex **1GaCl** was 0.12 and 0.17 in DMSO and water, respectively. In complex **1Zn,** the fluorescence emission peak appeared at 684 nm in both solvents and ΦF was 0.15 and 0.17 in DMSO and water, respectively. These spectroscopic properties of cationic Pcs **1GaCl** and **1Zn** in DMSO and water are characteristic for monomeric Pc complexes in solution [1,26,31–36]. In the measurements of the UV–vis spectra in PBS solution at a 1.5×10^{-5} M concentration, the sharp Q-band absorption of complex **1GaCl** was observed at 679 nm. However, the Q-band absorption for **1Zn** was observed at 631 and 666 nm as broadening bands. The broadening Q-bands of **1Zn** indicate the formation of aggregates. Aggregated Pcs exhibit limited applicability in photocatalysis because the aggregates convert electronic excitation energy into vibrational energy, due to the closeness of the individual molecules, thereby reducing the excited state lifetimes of Pcs and the ability to generate singlet oxygen [37,38].

In a PBS solution, **1GaCl** formed no aggregates owing to the effect of

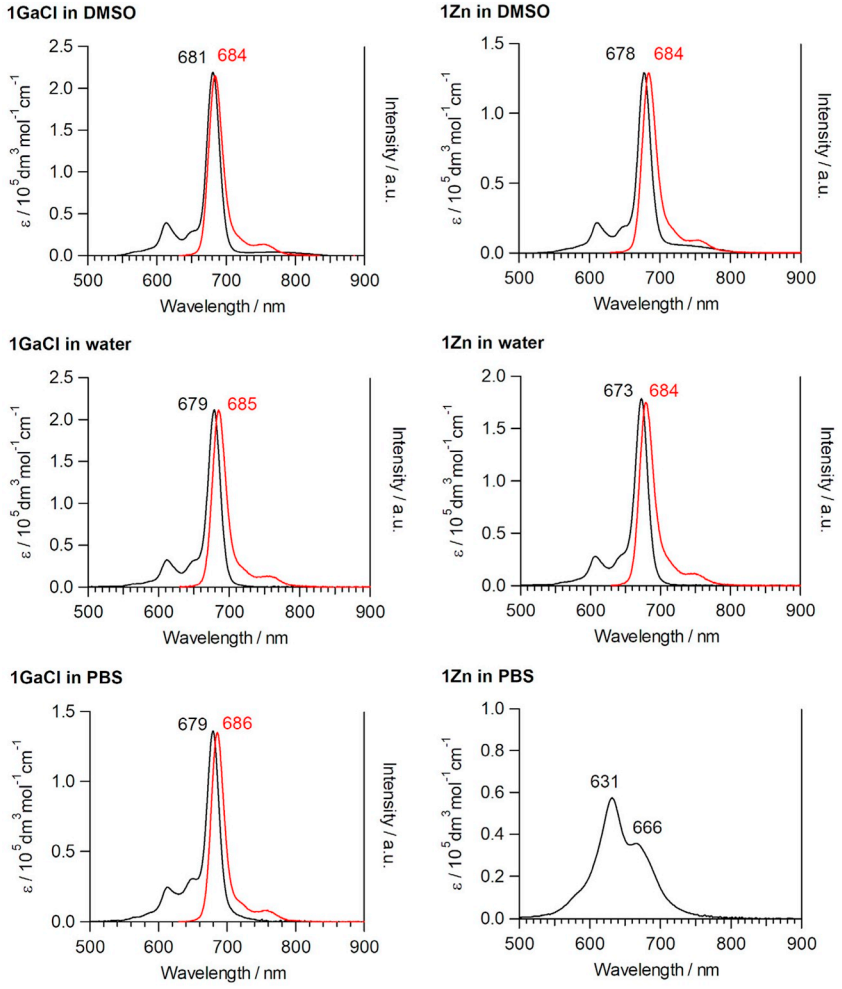

Fig. 2. Absorption and fluorescence spectra of complex **1GaCl** and **1Zn** in DMSO, water and PBS.

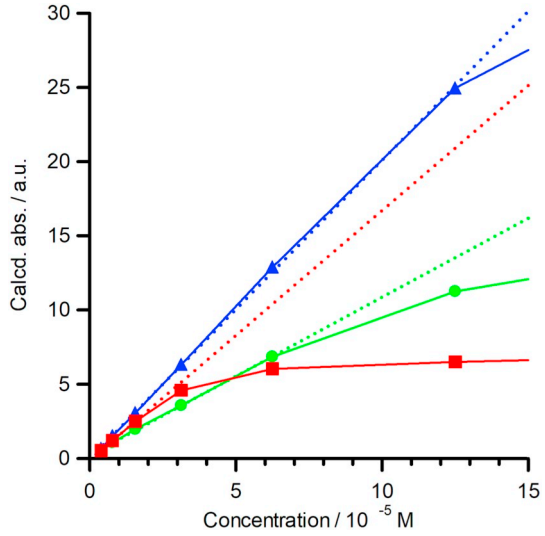

Fig. 3. Aggregation behavior of complex **1GaCl** and **1Zn** in water and PBS. ▲ show the absorbance of 1 GaCl in water, ● show the absorbance of 1 GaCl in PBS and ■ show the absorbance of 1 Zn in water.

Table 1
Photophysical and photochemical parameters of complex **1GaCl** and **1Zn**.

Pc	Solvent	λ_{Max} (nm)	λ_{Em} (nm)	SS (nm)	Φ_F[a]
1GaCl	DMSO	681	684	3	0.12
	Water	679	685	6	0.17
	PBS	679	686	7	0.14
1Zn	DMSO	678	684	6	0.15
	Water	673	684	11	0.17
	PBS	631, 666	–	–	–

[a] ΦF were evaluated using an absolute PL quantum yield measurement apparatus described in the literature [52].

steric hindrance between the peripheral groups and the Cl atom, being its axial ligand. As mentioned above, the formation of aggregates decreases the ability of the Pc to generate singlet oxygen, therefore the exploration of the concentrations that lead to aggregate formation is very significant. Therefore, the aggregation behavior induced by the concentration of complexes **1GaCl** and **1Zn** in aqueous media was investigated. The results of the aggregation behavior investigations are shown in Fig. 3 and S3, respectively. In the investigations of the aggregation behavior, quartz cells with cell length of 10 mm, 1 mm,

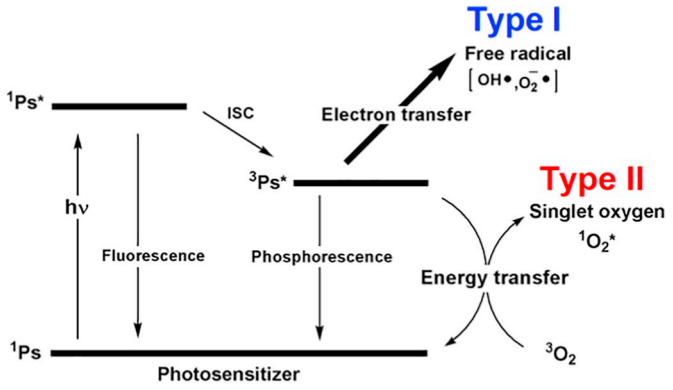

Scheme 2. The reaction mechanism of PDT.

0.1 mm were used. The absorbance values were calculated on the basis of the absorbance of quartz cell with cell length of 10 mm.

The cationic **1GaCl** strictly follows the Lambert-Beer law up to 1.2×10^{-4} M in water and 6.0×10^{-5} M in a PBS solution. On the other hand, cationic **1Zn** follows the Lambert-Beer law up to 1.5×10^{-5} M in water. However, **1Zn** remains aggregated in a PBS solution. These results reveal that complex **1GaCl** has high solubility and non-aggregation behavior in aqueous media, and that the introduction of an axial ligand (Cl) largely affects the solubility and aggregation behavior of metallo-Pcs, in agreement with previous studies [23]. While a number of cationic PBS-soluble Pcs are known, **1GaCl** is the first cationic Pc that shows no aggregation even at high concentrations in a PBS solution [39–45]. The fluorescence emission peak of complex **1GaCl** also appeared at 686 nm in a PBS solution. The absolute fluorescence quantum yield (ΦF) of complex **1GaCl** was determined to be 0.14 in a PBS solution. These values are characteristic of Pcs [46–51]. The results of the UV–vis and fluorescence spectra of cationic Pc complexes are listed in Table 1.

3.3. ESR measurement

Scheme 2 shows the two reaction mechanisms that lead to ROS formation in PDT. The two reaction mechanisms are distinguished according to the reactive oxygen species (ROS) which attacks the tumor cells. The Type I reaction leads to the formation of free radicals such as the superoxide anion radical ($O_2^{-}\cdot$) and the hydroxyl radical (OH·). The Type II reaction leads to the formation of singlet oxygen [8,9,53]. The generation of ROS is critical in the evaluation of the potential photosensitizers for PDT, **1GaCl** and **1Zn**. The generated ROS were identified by ESR measurements. 2,2,6,6-Tetraethyl-4-piperidone (4-Oxo-TEMP) was used as a spin trap reagent of singlet oxygen. 4-Oxo-TEMP and singlet oxygen react to generate 2,2,6,6-tetraethyl-4-piperidone- *N*-oxy-radical (4-Oxo-TEMPO). 4-Oxo-TEMPO can be identified by ESR measurement, because 4-Oxo-TEMPO has a nitroxide radical. The detection of 4-Oxo-TEMPO provides evidence of generation of singlet oxygen. The obtained ESR spectra are shown in Fig. 4. When the mixed DMSO solution of complex **1GaCl** and 4-Oxo-TEMP was irradiated, an ESR spectrum of triplet peaks with g = 2.014, 2.006 and 1.997, characteristic of a nitroxide radical, was observed. The obtained ESR spectrum is consistent with the reported ESR spectrum of the nitroxide radical. The irradiation of the mixed DMSO solution of cationic **1GaCl** and 4-Oxo-TEMP formed 4-Oxo-TEMPO [54–57]. To obtain additional evidence of the generation of singlet oxygen, 1,4-diazabicyclo[2,2,2]octane (DABCO) was added to the mixed DMSO

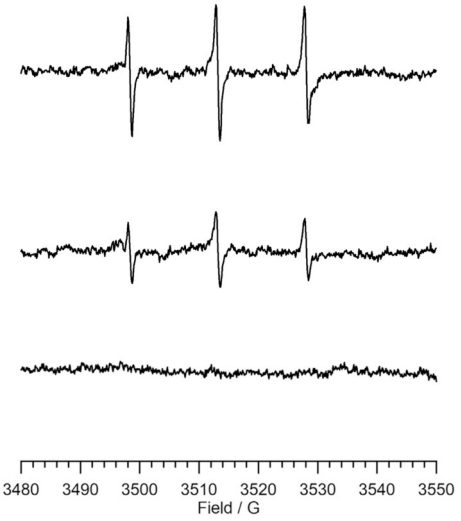

Fig. 4. Photo induced ESR spectra. Top: mixed DMSO solution of **1GaCl** and TEMP on light. Middle: sample solution added DABCO. Bottom: sample solution on dark.

solution of cationic **1GaCl** and 4-Oxo-TEMP. DABCO is known as a specific scavenger of singlet oxygen [58]. The irradiation of the mixed DMSO solution of complex **1GaCl** and 4-Oxo-TEMP with DABCO induced the decrease of the intensity of the ESR spectrum derived from 4-Oxo-TEMPO.

Under similar conditions, cationic **1Zn** also showed a similar ESR spectrum derived from 4-Oxo-TEMPO. These results indicate that complexes **1GaCl** and **1Zn** can generate singlet oxygen through irradiation.

3.4. Singlet oxygen generation properties

The ability of **1GaCl** and **1Zn** for generating singlet oxygen ($^1O_2$) upon light irradiation via a Type II reaction mechanism of PDT were evaluated. In the PDT reaction mechanism, multiple factors, including the triplet state lifetime of the photosensitizer, the singlet oxygen quenching abilities of the substituents and solvent, the efficiency of energy transfer between the photosensitizer and the oxygen molecules, and the probability of collision of molecules affect the process of PDT reactions [8–10].

The absolute quantum yields ($\Phi\Delta_{absolute}$) obtained from the oxidative decomposition of a scavenger by the singlet oxygen generated through photoirradiation of the Pc complexes were used as indicators for $^1O_2$ generation. The $\Phi\Delta_{absolute}$ was determined by a chemical method using the singlet oxygen scavengers, DPBF and ADMA. The $\Phi\Delta_{absolute}$ was calculated using Eq. (1) taking into account the number of molecules of decomposed scavenger and the photon number absorbed by the photosensitizer. The observed changes in the UV–vis spectra during irradiation for mixed solutions of each complex, **1GaCl** or **1Zn,** and scavenger are shown in Fig. 5.

The values of the $\Phi\Delta_{absolute}$ of Pc complexes are listed in Table 2. In the reaction between complex **1GaCl** and DPBF in a DMSO solution, the absorption band at around 417 nm due to DPBF significantly decreased during photo irradiation. This result indicated that the irradiation for the **1GaCl** induces the generation of $^1O_2$ and decomposition of DPBF. The value of $\Phi\Delta_{absolute}$ of complex **1GaCl** for DPBF in DMSO was calculated to be 4.4%. A similar spectral change was observed in the

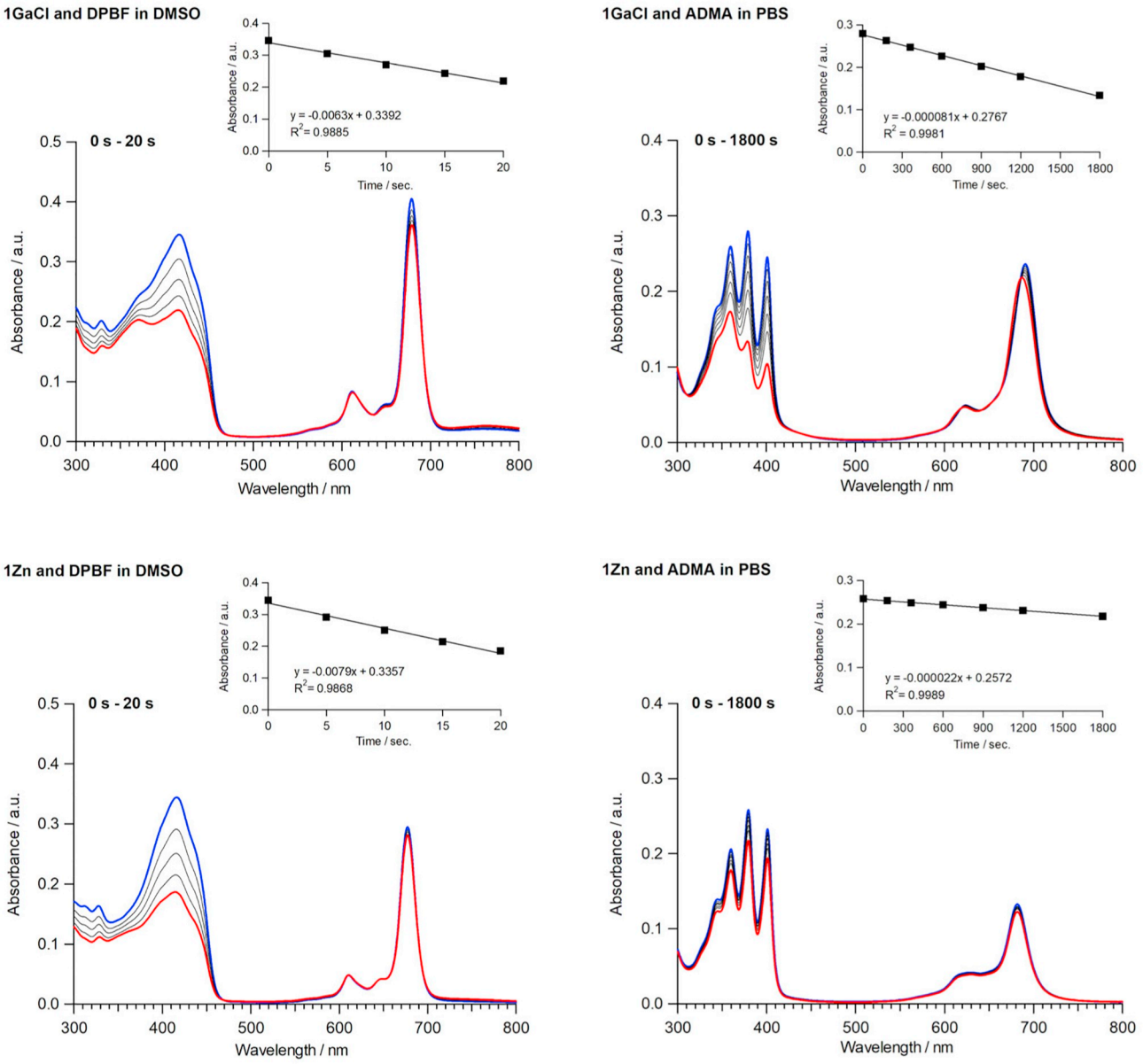

Fig. 5. The absorption spectral changes of **1GaCl** and **1Zn** during photo irradiations. (inset: the plots of absorbance of DPBF at 417 nm or ADMA at 380 nm versus time.)

Table 2
The values of the absolute quantum yields ($\Phi\Delta_{absolute}$).

Pc	Scavenger	Solvent	$\Phi\Delta_{absolute}$ [%]	$\Phi\Delta_{relative}$ [%]
1GaCl	DPBF	DMSO	4.4	29
	ADMA	PBS	0.029	–
1Zn	DPBF	DMSO	5.3	34
	ADMA	PBS	0.0090	–
ZnPc	DPBF	DMSO	10.3	67[a]
GaClPc	DPBF	DMSO	6.5	42

[a] Data from reference [47].

Table 3
Cytotoxicity IC_{50} values for **1GaCl** and **1Zn**. (CellTiter Blue assay, 1.5 J/cm^2).

Pc	Dark toxicity (IC_{50}, μM)	Photocytotoxicity (IC_{50}, μM)
1GaCl	> 100	> 100
1Zn	> 100	5.3

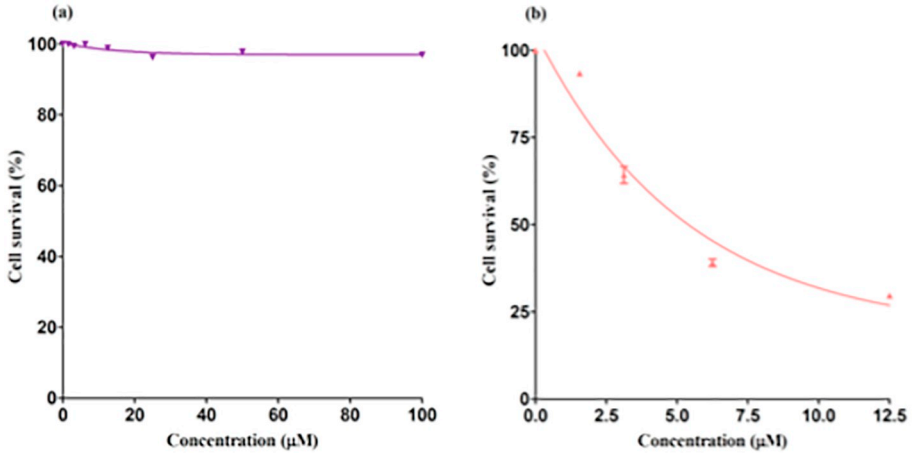

Fig. 6. Photocytotoxicity of 1GaCl (a) and 1Zn (b) in HEp2 cells using 1.5 J·cm^{-2} light dose.

reaction between complex **1Zn** and DPBF in a DMSO solution, which indicates that complex **1Zn** also generates $^1O_2$ and decomposes DPBF. The value of $\Phi\Delta_{absolute}$ of complex **1Zn** for DPBF in DMSO was even higher, 5.3%. Under the same conditions, the $\Phi\Delta_{absolute}$ values for non-substituted zinc phthalocyanine (ZnPc) and gallium phthalocyanine (GaClPc) are 10.3 and 6.5%, respectively. The comparison of the $\Phi\Delta_{absolute}$ values for the non-substituted metallo-Pcs and those of synthesized cationic **1GaCl** and **1Zn** shows that the $\Phi\Delta_{absolute}$ values for **1GaCl** and **1Zn** are smaller than those for the non-substituted metallo-Pcs. The smaller $\Phi\Delta_{absolute}$ values obtained for complexes **1GaCl** and **1Zn** could be caused by the energy loss due to the vibration of the peripheral substituents.

We also calculated the relative quantum yields ($\Phi\Delta_{relative}$) from the oxidative decomposition of DPBF through photo irradiation of the cationic **1GaCl** and **1Zn** using a standard value. The standard value used was $\Phi\Delta_{std.}$ = 67% for the oxidative decomposition of DPBF through photo irradiation of non-substituted ZnPc [47]. The calculation method for $\Phi\Delta_{relative}$ was the method previously described in the literature [26]. The values obtained for $\Phi\Delta_{relative}$ of **1GaCl** and **1Zn** for DPBF in DMSO were 29% and 34%, respectively. These $\Phi\Delta_{relative}$ values for **1GaCl** and **1Zn** are similar to those reported for non-aggregated Pc complexes having similar substituents in DMSO [26,31,32,49,59].

In the reaction between complex **1GaCl** and ADMA in a PBS solution, the decrease of only the absorption band due to ADMA at around 380 nm was observed during photo irradiation. In the reaction between complex **1Zn** and ADMA in a PBS solution, the Q-band derived from **1Zn** also changed in comparison with the observed Q-band of **1Zn** in PBS. This change could be due to the coordination of ADMA to the Zn atom of this Pc. By coordination with ADMA, the aggregation behavior of **1Zn** became weak, and **1Zn** showed a Q-band typical of a monomeric species. The decrease in the absorption band due to ADMA at around 380 nm also was observed.

The determined $\Phi\Delta_{absolute}$ values for complexes **1GaCl** and **1Zn** for ADMA in a PBS solution were 0.029 and 0.009%, respectively. These results indicate that both complexes **1GaCl** and **1Zn** can generate $^1O_2$ in a PBS solution. Thus, complexes **1GaCl** and **1Zn** are expected to be promising photosensitizers for PDT.

3.5. Cell study

The dark toxicity and photocytotoxicity of the complexes 1GaCl and 1Zn were evaluated in human carcinoma HEp2 cells using the Cell Titer Blue assay, and the results of these studies are summarized in Figs. S4, 6, and Table 3. The dark toxicity results in Fig. S2 show that both 1GaCl and 1Zn are nontoxic toward HEp2 cells in the dark. Various concentrations up to 100 μM were evaluated in this study. On the other hand, the two complexes showed distinct properties upon photo-irradiation with a low light dose of approximately 1.5 J/cm^2, as shown in Fig. 6. While 1GaCl exhibited no photocytotoxicity up to 100 μM, 1Zn was highly phototoxic, with a determined IC_{50} = 5.3 μM from the dose-response curves. This IC_{50} value is within the same range of values previously reported for cationic Pcs bearing pyridyloxy groups [23]. In the case of 1Zn, the combination of low dark cytotoxicity, high photocytotoxicity and effective generation of $^1O_2$ in a PBS solution suggest that this compound is very promising as a photosensitizer for PDT applications.

Aiming to determine the cause of the high photocytotoxicity observed for 1Zn, the preferential sites of intracellular localization of 1GaCl and 1Zn were evaluated in human carcinoma HEp2 cells using fluorescence microscopy. The results of these studies are shown in Figs. 7 and 8 for 1GaCl and 1Zn, respectively, and summarized in Table 4. These studies were performed using the organelle-specific probes ER Tracker Blue/White (ER), BODIPY Ceramide (Golgi), Mito-Tracker Green (Mitochondria), and LysoTracker Green (Lysosomes), and then merging the fluorescent images of these probes with the fluorescent images of the photosensitizers 1GaCl or 1Zn. As shown in Figs. 7 and 8, the overlay of these images revealed that both 1GaCl and 1Zn were found to localize in multiple organelles within the cell, including the ER, Golgi apparatus, lysosomes and the mitochondria. However 1Zn was observed in greater amounts in the ER, Golgi, and lysosomes indicating that this compound is more efficient at cellular internalization and localization in organelles that are important targets for PDT-induced cell death.

4. Conclusion

The cationic Pcs 1GaCl and 1Zn bearing eight *N*-methyl-(4-methylpyridinium-3-yloxy) groups around the Pc macrocycle were synthesized. The obtained cationic Pcs were highly soluble in DMSO, moderately soluble in water and PBS solutions. In a PBS solution, 1GaCl formed no aggregates owing to the effect of steric hindrance between the peripheral groups and the Cl atom, being its axial ligand. The cationic 1GaCl is the first cationic Pc that shows no aggregation even at high concentrations in a PBS solution. The cationic Pcs 1GaCl and 1Zn

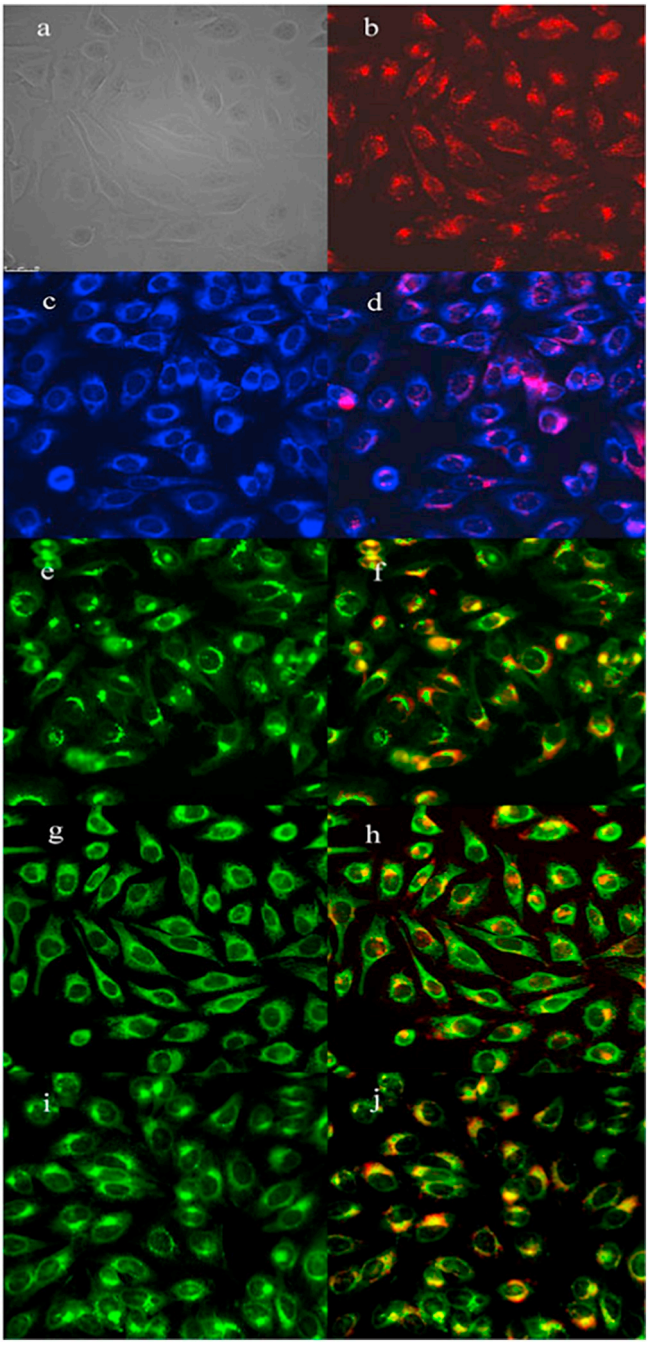

Fig. 7. Subcellular localization of 1GaCl in HEp2 cells at 10 μM for 6 h. (a) Phase contrast, (b) the fluorescence of 1GaCl, (c) ER Tracker Blue/White, (d) overlay of 1GaCl and ER Tracker, (e) BODIPY Ceramide, (f) overlay of 1GaCl and BODIPY Ceramide, (g) MitoTracker Green, (h) overlay of 1GaCl and MitoTracker, (i) LysoSensor Green, and (j) overlay of 1GaCl and LysoSensor Green. Scale bar: 0–25 μm.

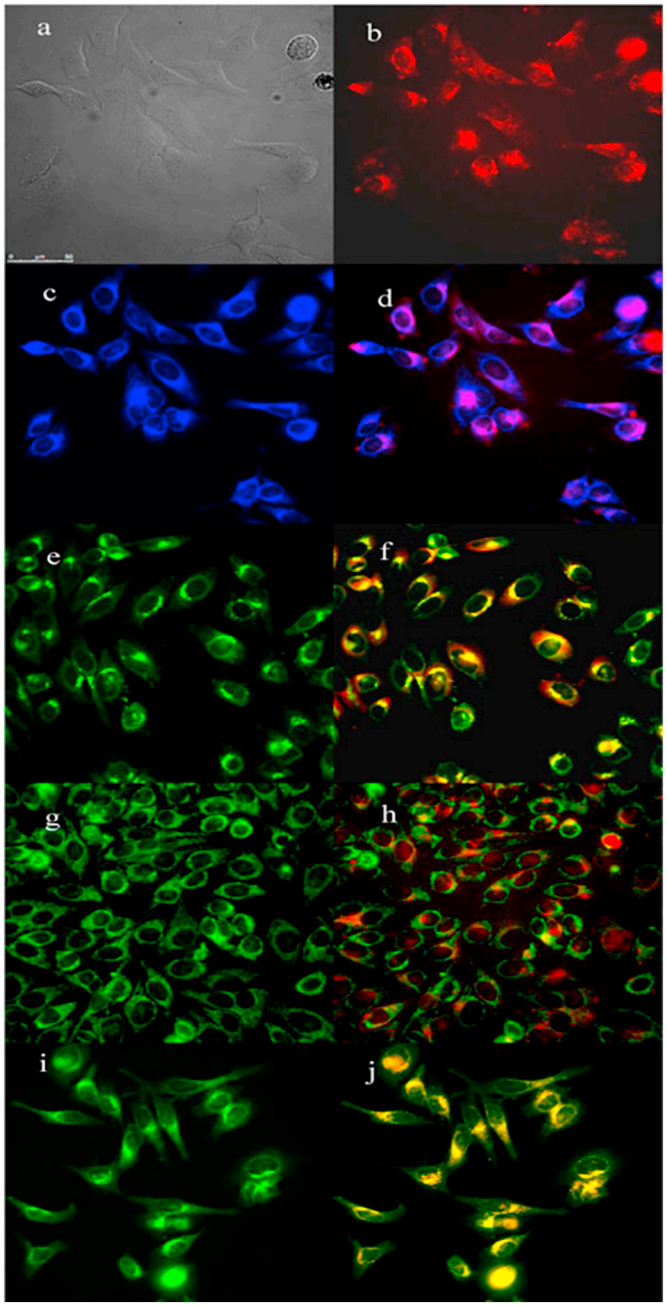

Fig. 8. Subcellular localization of 1Zn in HEp2 cells at 10 μM for 6 h. (a) Phase contrast, (b) the fluorescence of 1Zn, (c) ER Tracker Blue/White, (d) overlay of 1Zn and ER Tracker, (e) BODIPY Ceramide, (f) overlay of 1Zn and BODIPY Ceramide, (g) MitoTracker Green, (h) overlay of 1Zn and MitoTracker, (i) LysoSensor Green, and (j) overlay of 1Zn and LysoSensor Green. Scale bar: 0–50 μm.

also exhibited singlet oxygen generation ability in DMSO and PBS solution. The absolute quantum yields ($\Phi\Delta_{absolute}$) for the photogeneration of singlet oxygen using 1GaCl and 1Zn have been determined to be 4.4 and 5.3%, respectively, in DMSO solution.

The cytotoxicity and intracellular sites of localization of 1GaCl and 1Zn were evaluated in human HEp2 cells. These studies showed that both compounds are not cytotoxic in the dark (IC_{50} > 100 mM) and localize intracellularly in multiple organelles, including the ER, Golgi apparatus, lysosomes, and to a smaller extent in the cell mitochondria. Upon exposure to a low light dose (1.5 J/cm^2), 1Zn revealed high phototoxicity in human HEp2 cells. This is probably due to its enhanced ability for cellular internalization and generation of singlet oxygen within cells. We concluded that 1Zn could have the potential of photosensitizer for PDT.

Table 4
Major (+ + +) and minor (+) subcellular sites of localization in HEp2 cells.

Pc	ER	Golgi	Mitochondria	Lysosomes
1GaCl	+ +	+ +	+	+ +
1Zn	+ + +	+ + +	+	+ + +

Acknowledgements

The authors are grateful to Ehime University for the crystallographic analysis. The authors are grateful to Ms. Michiko Egawa (Shimane University) for her measurements of elemental analysis. The X-ray diffraction experiment was performed at Advanced Research Support Center, Ehime University. Thanks are due to the Research Center for Molecular-Scale Nanoscience, the Institute for Molecular Science (IMS), Okazaki, Japan.

Appendix A. Supplementary data

Supplementary data to this article can be found online at https://doi.org/10.1016/j.jinorgbio.2018.11.013.

References

[1] J. Mack, N. Kobayashi, Chem. Rev. 111 (2011) 281–321.
[2] G. Torre, P. Vázquez, F. Agulló-López, T. Torres, Chem. Rev. 104 (2004) 3723–3750.
[3] G. Bottari, G. Torre, D.M. Guldi, T. Torres, Chem. Rev. 110 (2010) 6768–6816.
[4] D.E.J.G.J. Dolmans, D. Fukumura, R.K. Jain, Nat. Rev. Cancer 3 (2003) 380–387.
[5] J. Zhao, W. Wu, J. Sun, S. Guo, Chem. Soc. Rev. 42 (2013) 5323–5351.
[6] R.A. Weersink, A. Bogaards, M. Gertner, S.R.H. Davidson, K. Zhang, G. Netchev, J. Trachtenberg, B.C. Wilson, J. Photochem. Photobiol. B Biol. 79 (2005) 211–222.
[7] W. Hu, M. Xie, H. Zhao, Y. Tang, S. Yao, T. He, C. Ye, Q. Wang, X. Lu, W. Huang, Q. Fan, Chem. Sci. 9 (2018) 999–1005.
[8] T.J. Dougherty, C.J. Gomer, B.W. Henderson, G. Jori, D. Kessel, M. Korbelik, J. Moan, Q. Peng, J. Natl. Cancer Inst. 90 (1998) 889–905.
[9] S. Yano, S. Hirohara, M. Obata, Y. Hagiya, S. Ogura, A. Ikeda, H. Kataoka, M. Tanaka, T. Joh, J Photochem Photobiol C: Photochem Rev 12 (2011) 46–67.
[10] S.B. Brown, E.A. Brown, I. Walker, Lancet Oncol. 5 (2004) 497–508.
[11] F. Dumoulin, M. Durmus, V. Ahsen, T. Nyokong, Coord. Chem. Rev. 254 (2010) 2792–2847.
[12] N.B. McKeown, Phthalocyanine Materials: Synthesis, Structure, and Function, Cambridge University Press, Cambridge, 1998.
[13] M.C. Derosa, R.J. Crutchley, Coord. Chem. Rev. 233–244 (2002) 351–371.
[14] M. Sonoda, C.M. Krishna, P. Riesz, Photochem. Photobiol. 46 (1987) 625–631.
[15] D.J. Ball, S.R. Wood, D.I. Vernon, J. Griffiths, T.M.A.R. Dubbelman, S.B. Brown, J. Photochem. Photobiol. B Biol. 45 (1998) 28–35.
[16] D.J. Ball, S. Mayhew, S.R. Wood, J. Griffiths, D.I. Vernon, S.B. Brown, Photochem. Photobiol. 69 (1999) 390–396.
[17] A. Minnock, D.I. Vernon, J. Schofield, J. Griffiths, J.H. Parish, J. Photochem. Photobiol. B Biol. 32 (1996) 159–164.
[18] A. Minnock, D.I. Vernon, J. Schofield, J. Griffiths, J.H. Parish, S.B. Brown, Antimicrob. Agents Chemother. 44 (2000) 522–527.
[19] I. Scalise, E.N. Durantini, Bioorg. Med. Chem. 13 (2005) 3037–3045.
[20] B. Mızrak, E.B. Orman, S. Abdurrahmanoglu, A.R. Ozkaya, J. Porphyrins Phthalocyanines 22 (2018) 243–249 iss.1-3.
[21] L. George, A. Hiltunen, V. Santala, A. Efimov, J. Inorg. Biochem. 183 (2018) 94–100.
[22] L. George, A. Muller, B. Roder, V. Santala, A. Efimov, Dyes Pigments 147 (2017) 334–342.
[23] H. Li, T.J. Jensen, F.R. Fronczek, M.G.H. Vicente, J. Med. Chem. 51 (2008) 502–511.
[24] D. Wöhrle, M. Eskes, K. Shigehara, A. Yamada, Synthesis (1993) 194–196.
[25] M. Durmus, A. Erdoğmus, A. Ogunsipe, T. Nyokong, Dyes Pigments 82 (2009) 244–250.
[26] M. Camur, V. Ahsena, M. Durmus, J. Photochem. Photobiol. A Chem. 219 (2011) 217–227.
[27] M. Haas, S. Liu, A. Neels, S. Decurtins, Eur. J. Org. Chem. (2006) 5467–5478.
[28] R. Kubiak, J. Janczak, M. Śledź, E. Bukowska, Polyhedron 26 (2007) 4179–4186.
[29] R. Fujishiro, H. Sonoyama, Y. Ide, S. Mori, T. Sugimori, A. Nagai, K. Yoshino, M. Nakamura, T. Ikeue, Heterocycles 94 (2017) 131–139.
[30] F. Yang, X. Fang, H. Yu, J. Wang, Acta Cryst C64 (2008) m375–m377.
[31] M. Durmus, V. Ahsen, J. Inorg. Biochem. 104 (2010) 297–309.
[32] M. Durmus, T. Nyokong, Inorg. Chem. Commun. 10 (2007) 332–338.
[33] X. Li, J. Guo, J. Zhuang, B. Zheng, M. Ke, J. Huang, Bioorg. Med. Chem. Lett. 25 (2015) 2386–2389.
[34] S. Makhseed, M. Machacek, W. Alfadly, A. Tuhl, M. Vinodh, T. Simunek, V. Novakova, P. Kubat, E. Rudolf, P. Zimcik, Chem. Commun. 49 (2013) 11149–11151.
[35] A. Atsay, A. Gül, M.B. Koçak, Dyes Pigments 100 (2014) 177–183.
[36] P. Zimcik, M. Miletin, H. Radilova, V. Novakova, K. Kopecky, J. Svec, E. Rudolf, Photochem. Photobiol. 86 (2010) 168–175.
[37] J. Liua, J. Li, X. Yuan, W. Wang, J. Xue, Photodiagn. Photodyn. Ther. 13 (2016) 341–343.
[38] V. Çakır, D. Çakır, M. Göksel, M. Durmuş, Z. Bıyıklıoglu, H. Kantekin, J. Photochem. Photobiol. A Chem. 299 (2015) 138–151.
[39] B. Zheng, M. Ke, W. Lan, L. Hou, J. Guo, D. Wan, L. Cheong, J. Huang, Eur. J. Med. Chem. 114 (2016) 380–389.
[40] D. Çakır, V. Çakır, Z. Bıyıklıoglu, M. Durmus, H. Kantekin, J. Organomet. Chem. 745-746 (2013) 423–431.
[41] V. Çakır, D. Çakır, M. Piskin, M. Durmus, Z. Bıyıklıoglu, J. Organomet. Chem. 783 (2015) 120–129.
[42] V. Çakır, D. Çakı, M. Pişkin, M. Durmuş, Z. Bıyıklıoglu, J. Lumin. 154 (2014) 274–284.
[43] M. Çamur, M. Durmus, M. Bulut, Polyhedron 41 (2012) 92–103.
[44] A.A. Esenpınar, M. Durmus, M. Bulutc, Spectrochim. Acta A 79 (2011) 608–617.
[45] J.B. Pereira, E.F.A. Carvalho, M.A.F. Faustino, R. Fernandes, M.G.P.M.S. Neves, J.A.S. Cavaleiro, N.C.M. Gomes, A. Cunha, A. Almeida, J.P.C. Tome, Photochem. Photobiol. 88 (2012) 537–547.
[46] S. Moeno, T. Nyokong, J. Photochem. Photobiol. A Chem. 215 (2010) 196–204.
[47] H. Yanık, D. Aydın, M. Durmus, V. Ahsen, J. Photochem. Photobiol. A Chem. 206 (2009) 18–26.
[48] N. Masilela, T. Nyokong, Dyes Pigments 84 (2010) 242–248.
[49] S. Moeno, T. Nyokong, J. Photochem. Photobiol. A Chem. 203 (2009) 204–210.
[50] J. Chen, Q. Gan, S. Li, F. Gong, Q. Wang, Z. Yang, S. Wang, H. Xu, J.S. Ma, G. Yang, J. Photochem. Photobiol. A Chem. 207 (2009) 58–65.
[51] A.T. Bilgiçli, M. Durdasoglu, E. Kırbaç, M.N. Yarasir, M. Kandaz, Polyhedron 100 (2015) 1–9.
[52] R. Sasai, N. Iyi, H. Kusumoto, Bull. Chem. Soc. Jpn. 84 (2011) 562–568.
[53] R. Gerdes, D. Wöhrle, W. Spiller, G. Schneider, G. Schnurpfeil, G. Schulz-Ekloff, J. Photochem. Photobiol. A Chem. 111 (1997) 65–74.
[54] Y. Lion, M. Delmelle, A.V. Vorst, Nature 263 (1976) 442–443.
[55] G. Nardia, I. Manet, S. Monti, M.A. Miranda, V. Lhiaubet-Vallet, Free Radic. Biol. Med. 77 (2014) 64–70.
[56] P. Niedbalski, C. Parish, A. Kiswandhi, L. Lumata, Magn. Reson. Chem. 54 (2016) 962–967.
[57] J.M. Buffa, M.A. Grela, M.I. Aranguren, V. Mucci, Carbohydr. Polym. 136 (2016) 744–749.
[58] S. Wei, J. Zhou, D. Huang, X. Wang, B. Zhang, J. Shen, Dyes Pigments 71 (2006) 61–67.
[59] D.O. Oluwole, F.A. Sarı, E. Prinsloo, E. Dube, A. Yuzer, T. Nyokong, M. Ince, Spectrochim. Acta A Mol. Biomol. Spectrosc. 203 (2018) 236–243.